Tribology Letters (2020) 68:36
https://doi.org/10.1007/s11249-020-1275-3

ORIGINAL PAPER

Study of Micro- and Nanoscale Wetting Properties of Lubricants Using AFM Force–Distance Curves

Sebastian Friedrich[1] · **Brunero Cappella**[1]

Received: 26 August 2019 / Accepted: 29 January 2020 / Published online: 12 February 2020

Abstract
Force–distance curves have been recorded on thin films of nine different lubricants to extend the results of a previous work of one of the authors. The lubricants wet the AFM tip, which causes a capillary force. This depends on the shape of the tip, as well as on properties of the lubricants such as surface tension, contact angle, and viscosity, which have been additionally measured with other methods. Thus, their influence on the shape of the curves could be analyzed. The main features of force–distance curves on different lubricants have been characterized and the underlying phenomena could be explained. Results contribute to a better understanding of fundamental mechanisms influencing lubrication and hence friction and wear at the micro- and nanoscale.

Keywords Lubricants · Atomic force microscopy · Force–distance curves

1 Introduction

Atomic force microscopy (AFM) plays an important role as a multifunctional tool in nanotribology. Mostly its scanning ability is employed, e.g., to perform topography scans to record the pre- and post-experiment morphology of tribological samples and analyze the wear track. Equipped with a diamond tip, it can also be used to perform scratch tests [1, 2]. Furthermore, through the measurement of the torsional deformation of the cantilever and of the lateral force during scanning in contact mode, the nanoscale friction on samples such as thin polymeric lubricants on solid substrates can be measured [3].

Polymeric lubricants form thin liquid films, which are employed to improve the friction and wear behavior of materials. While lubrication is a macroscopic property, it is governed by interactions in the micro- and nano-range. A method to study the properties of such lubricant films in detail are force–distance curves with AFM [4–8]. Examples of applications are measurements on hard disk drives, with the AFM tip mimicking the slider, and on residual lubricant layers on working pieces, e.g., to test the efficiency of cleaning procedures. In the first studies by Mate et al., AFM has been used to determine the disjoining pressure, the meniscus force, the topography of the liquid film, the molecular conformation, as well as the film thickness with nanometer precision [9, 10]. Those methods have been refined and adapted for thicker films by Bowles et al. [11, 12]. Capillary forces have been identified as the dominating interaction. Force-distance curves have further been used to systematically study the adhesive forces between lubricated carbon surfaces and the AFM tip depending on the surface energy, molecular polarity of the lubricant, and loading rate [13, 14]. Studies have also been able to distinguish the adsorption properties of different lubricants to hard disk surfaces [15] and to deduce the structure of an anti-wear film [3]. Molecular layering has been observed for polyalphaolephins and an ester [16], as well as for ionic liquids [17], which are typical lubricant constituents.

Those cited studies concern very thin films from submonolayer coverage to a few tens of nanometers. Ally et al. have extended this range to films with thickness of several micrometers, which have been indented with a polystyrene microsphere attached to the AFM cantilever [18]. Thereby, they have shown that the interaction depends on the surface tension and the viscosity of the lubricant. For a given lubricant, the force acting on the cantilever depends only on the perimeter of the three-phase contact line between AFM tip, lubricant, and air.

✉ Brunero Cappella
brunero.cappella@bam.de

[1] Federal Institute for Material Research and Testing (BAM), Unter den Eichen 87, 12205 Berlin, Germany

Cappella has proven this result and has found that curves acquired on films of different thickness, at different velocities, or with different dwell times consequently all have the same shape when the distance axis is rescaled [19]. This work has also provided insights into the dynamics of tip-wetting. The tip is initially wetted by indenting the lubricant, after which the lubricant immediately forms a meniscus, which causes an attractive capillary force. This capillary force $F(H)$, where H is the distance between the tip apex and the three-phase contact line, is caused by the surface tension γ and is given by

$$F(H) = p(H)\gamma \sin\alpha \tag{1}$$

with the perimeter of the three-phase contact line $p(H)$. Geometrical quantities are shown in Fig. 1. The angle α is given by $\alpha = \frac{\pi}{2} + \beta - \theta$, where β is the half aperture of the tip cone, and θ is the contact angle between lubricant and tip. Further details about the calculation of this force can be found in Refs.[18, 19], and in the references therein.

Cappella has shown that the force depends on the height of the wetted portion of the tip, H, and not on the distance between the tip apex and the rest position of the liquid–air interface, S (see Fig. 1). It is important to discriminate both variables. While S is the quantity measured directly through force distance curves, H cannot be measured during the acquisition. H may be larger or smaller than S if the lubricant wets the tip and the three-phase contact line climbs up, or the lubricant does not wet the tip and the three-phase contact line is pushed back. Because of this discrepancy, force–distance curves on films of different thickness, or curves recorded with different scan rate or dwell time, initially do not overlap, although the force depends only on the tip shape. Only when the distance axis is rescaled to take the wetted portion of the tip, H, into account, those curves overlap.

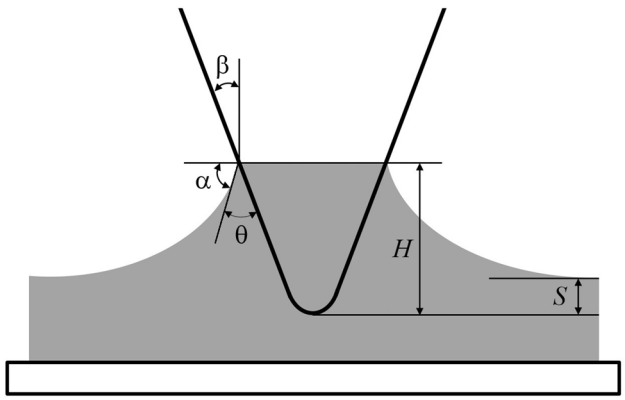

Fig. 1 Schematic representation of the AFM-tip in the lubricant. The angle β is the half aperture of the tip cone, θ is the contact angle between lubricant and tip, and α is given by $\alpha = \pi/2 + \beta - \theta$. S is the distance between the tip apex and the rest position of the lubricant surface; H is the distance between the tip apex and the three-phase-contact line

The study of Cappella [19], as well as most other studies cited above [9–15], have exclusively used perfluoropolyethers (PFPEs) as lubricants. The present study extends the investigation to a group of nine lubricants of different types. The aim is to verify the findings on PFPE for other lubricants and to analyze the dependence of the shape of force-distance curves on various material properties of the lubricant and on the tip shape, thus confirming Eq. 1.

The presented measurements shed light on mechanisms influencing lubrication at the micro- and nanoscale, since the AFM-tip can be considered as an asperity. Characterizing the dynamic wetting of the AFM-tip means to gain insight into the actual lubrication of asperities, which play a fundamental role in friction and wear processes, most of all in the running-in regime.

2 Material and Methods

2.1 Materials

Nine different lubricants have been used in this study. They are listed in Table 1. Among them are both research chemicals and commercial lubricants. For the measurements, a drop of the liquid was put on a glass microscope slide, which has been previously cleaned and rinsed with acetone. The drop was then wiped off with another piece of glass slide, or with a Kimwipe, to obtain a thin film in the nano- to micro-range.

2.2 Atomic Force Microscopy

Force–distance curves have been acquired with a Cypher AFM (Asylum Research, Oxford Instruments, Santa Barbara, USA). For all measurements, Nanosensors PPP-FMAuD cantilevers (NanoWorld, Neuchatel, Switzerland) have been used. They are made of silicon with a reflective gold coating on the back side to enhance the reflectivity of the laser beam. Before the measurements, the cantilevers have been calibrated against a hard surface (glass) to obtain the inverse optical lever sensitivity. The spring constant k_c could then be obtained from the thermal noise spectrum [20]. Hooke's law $F = -k_c\delta$ allows to calculate the force F which acts on the cantilever from the deflection δ.

Before and after each measurement a TGT1 test grating (NT-MDT Spectrum Instruments, Moscow, Russia) consisting of an array of sharp tips has been scanned. The resulting image is a replica of the AFM tip [21, 22] and has been used to measure the perimeter of the tips as a function of the distance from the apex. The cantilevers

Table 1 Overview of lubricants used in this study

Name	Type	Surf. tension	Cont. angle	Viscosity
Squalane	Hydrocarbon (HC)	28.4	18.9°	28
Paraffin viscous	Hydrocarbon (HC)	31.0	24.9°	97
Halocarbon oil 27	Polychlorotrifluoroethylene (PCTEF)	27.7	22.1°	116
Halocarbon oil 700	Polychlorotrifluoroethylene (PCTEF)	28.9	45.9°	3850
Fomblin	Perfluoropolyether (PFPE)	18.2	34.7°	207
Lupranol VP 9209	Polyalkylene glycol (PAG)	44.3	39.5°	270
Plurasafe WI 1715	Polyalkylene glycol (PAG)	32.6	27.4°	514
50-HB-55	Polyalkylene glycol (PAG)	30.9	13.3°	14
Emkarate	Polyolester (POE)	31.8	13.1°	32

Surface tension is given in mN/m, and dynamic viscosity in mPa·s at a temperature of 25 °C. Squalane and Paraffin have been purchased from Merck (Darmstadt, Germany), Halocarbon Oil 27, Halocarbon oil 700, and Fomblin from Sigma-Aldrich (St. Louis, USA), Lupranol and Plurasafe from BASF (Ludwigshafen, Germany), 50-HB-55 from DowDuPont (Wilmington, USA), and Emkarate from CPI (Wickliffe, USA)

used in this study have a spring constant of 3.7 ± 0.1 N/m and a half cone angle of $29.2 \pm 0.6°$.

2.3 Surface Tension Measurements

The surface tension of all lubricants has been measured through the Wilhelmy plate method using a K100 MK2 Tensiometer (Krüss, Hamburg, Germany). A standard rough platinum plate with a wetted length of 40.16 mm, which has been glowed in a propane/butane flame before the measurement, has been used. The dipping depth was 2 mm.

2.4 Contact Angle Measurements

The contact angle of all lubricants on a silicon wafer has been measured with a DSI 30 drop shape analyzer (Krüss, Hamburg, Germany). Measurements have been conducted manually with sample volumes of 1–3 µl. The drop shape was fitted with an ellipse with the baseline determined manually.

2.5 Viscosity Measurements

The dynamic viscosity of all lubricants used in this work has been measured with an MCR 300 rheometer (Anton Paar, Graz, Austria). A CC 27 cylinder measuring system with a liquid height of 5 mm and a sample volume of 25–30 ml has been used. The temperature has been set to 25 °C with a Peltier element. 30 values have been recorded with 5 s measuring time each, while increasing the shear rate from 1 to 1000 1/min and subsequently decreasing it again. The lubricants behave approximately Newtonian, so representative values at intermediate shear rates are given here as results.

3 Results

Figure 2 shows the different parts of an exemplary force distance curve on a lubricant film, in this case Emkarate. The approach curve is grey, and the retraction curve is black, as indicated by the red arrows. At large separation between tip and lubricant the deflection is zero. By decreasing the distance, when the attractive force between tip and lubricant overcomes the elastic force of the cantilever, a "jump-to-contact" occurs and the cantilever deflects downward. The jump-to-contact is due to an attractive (negative) capillary force between the tip and the lubricant, which increases as the tip is moved further towards the glass substrate. As soon as the tip touches the substrate, the cantilever deflects upward due to a repulsive (positive) force. The thickness of the lubricant layer is calculated as the difference in piezo extension between the jump-to-contact and the onset of the repulsive force, plus the cantilever deflection at this onset. After the repulsive force has reached a certain value (the "trigger point"), the tip is retracted again. It first loses contact with the solid substrate.

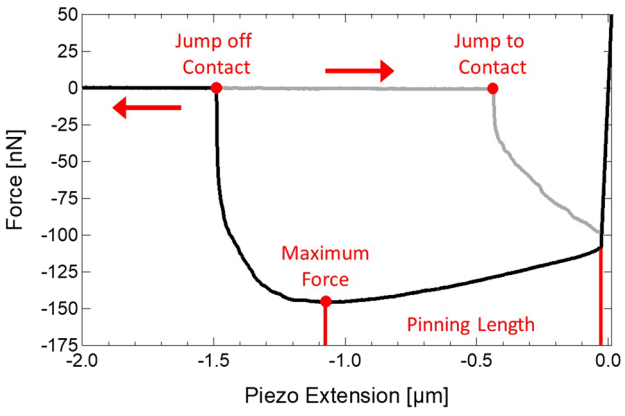

Fig. 2 Exemplary force-distance curve on Emkarate highlighting the different parts of the curve. The approach and retraction curves are displayed in grey and black, respectively

Although the tip is retracted, the attractive (or adhesive) force increases over a certain distance. The interval in the force–displacement curve between the detachment from the substrate and the point of maximum attractive force is defined in the following as "pinning length". In this regime the three-phase contact line is pinned to the tip, which means that it does not move. From the point of maximum force onward, the lubricant detaches from the tip, the contact line withdraws, and the force decreases and reaches zero at the "jump-off-contact".

The aim of this study is to compare force–distance curves on thin films of different lubricants. Curves on Fomblin have already been described in Ref.[19]. In the present work, measurements on nine lubricants have been performed, while the same tip was used for three groups of four lubricants at a time. Exemplary force curves on films of approximately 400 nm thickness are shown in Fig. 3. For the sake of clarity, approach and retract curves are not overlapped. Instead, approach corresponds to negative piezo extension, and retract corresponds to positive piezo extension. It has been shown for Fomblin that the shape of the curve depends only on the tip perimeter, the lubricant surface tension, and the contact angle between lubricant and tip [19]. The same tip has been used for all curves in each of Fig. 3a–c, respectively. The perimeter of the cross-section of the tips at a certain distance from the apex, measured by scanning a TGT1 test grating in Tapping Mode at different stages of the measurement, is shown in Fig. 3d–f. It shows little variation throughout the measurement series. However, the shape of the curves in Fig. 3a–c is very different for different lubricants, which indicates that they possess very different wetting behaviors. This depends on properties like the viscosity. The curves differ in their maximum attractive force both during approach and retract, as well as in the retraction length before the jump-off contact, and the pinning length. Those quantities will be analyzed in more detail later.

Before going over to the analysis of the curves, since the same tip has been used for measurements of groups of four lubricants at a time, it is necessary to examine the possible contamination of the tip.

The contamination of the tip with lubricants can be excluded, at least for the materials employed in this work.

First of all, after each force-distance measurement, the tip has been scanned in Tapping Mode on a test grating to measure the perimeter. During the scan, thin liquid films or single drops, which might have adhered on the tip, adsorb on the grating. Otherwise, because of the strong adhesion of liquid materials, the tip would stick on the grating surface and a scanning in Tapping Mode would not be possible [18].

Second, measurements on Fomblin have been performed with all three tips, but in different succession: in the first group (Fig. 3a), Fomblin was the first lubricant, in the second (Fig. 3b), it was the second, after paraffin, and in the third (Fig. 3c), it was the third one, after the two halocarbons. Yet, when calculating $F(H)/p(H) = \gamma \sin \alpha$ (see Eq. 1), the three measurements on Fomblin yield exactly the same values, showing definitely that the force is determined by the interaction between Fomblin and silicon and that no intermediate film of any lubricant, which would influence the interaction and the values of $\gamma \sin \alpha$, is present.

3.1 Rescaling and Overlapping

A crucial finding of Ref [19] was that force–distance curves acquired on Fomblin with varying dwell time, acquisition rate, or film thickness can be overlapped after a rescaling of the x-axis (piezo extension or time). To verify this for other lubricants, the respective measurements have been performed on all nine lubricants. They are exemplarily shown for Squalane in Fig. 4 and are similar for all other lubricants. Figure 4a shows curves with dwell times between 0 and 10 s (0 to 2 s in steps of 0.1 s and 2 to 10 s in steps of 1 s). In those measurements, the tip is not immediately retracted when the trigger point has been reached. Instead, it is left to dwell while in contact with the substrate for a given time. The approach curves are shown in blue. Because the approach is not affected by the dwell, those curves are nearly the same. The little variation for large dwell times is caused by liquid flow during the recording of the first curves and to subsequent increase of the thickness of the film. While the tip dwells on the substrate, the lubricant climbs up the tip. This results in a larger attractive force and longer curves when the tip is retracted, as can be seen in the red retraction curves. With no dwell time, the maximum adhesive force is 77 nN, and the piezo is retracted by 590 nm before the meniscus breaks. With 10 s dwell time, the maximum adhesive force increases to 126 nN, and the rupture of the meniscus takes place at 810 nm. As in the case of Fomblin, also those curves can be overlapped after being rescaled in x-direction, as shown in Fig. 4b. The rescaling factors are shown in Fig. 4f vs the contact time. However, the part of the curves that can be overlapped is limited to the section between the point of maximum force and the jump-off-contact. The part where pinning is present cannot be overlapped. This is a new finding, because the pinning length of Fomblin, the only lubricant used in the previous study of Cappella [19], is insignificant.

Besides varying the dwell time, another way to influence the time the tip spends in the lubricant during the force–distance curve is varying the acquisition time (inverse of the scan rate). Figure 4c shows approach (blue) and retraction (red) curves taken at scan rates between 0.01 and 10 Hz (0.01 Hz, 0.02–0.1 Hz in steps of 0.02 Hz, 0.1–1 Hz in steps of 0.1 Hz, 1–10 Hz in steps of 1 Hz). The maximum attractive force increases already in the approach curves from 50 to 130 nN as the scan rate is decreased. This is due to the longer time the tip spends in the lubricant, during which the lubricant climbs up the tip. The upwards movement of the three-phase contact line induces an increase of the force on the cantilever. Accordingly, the retraction curves reach larger attractive forces

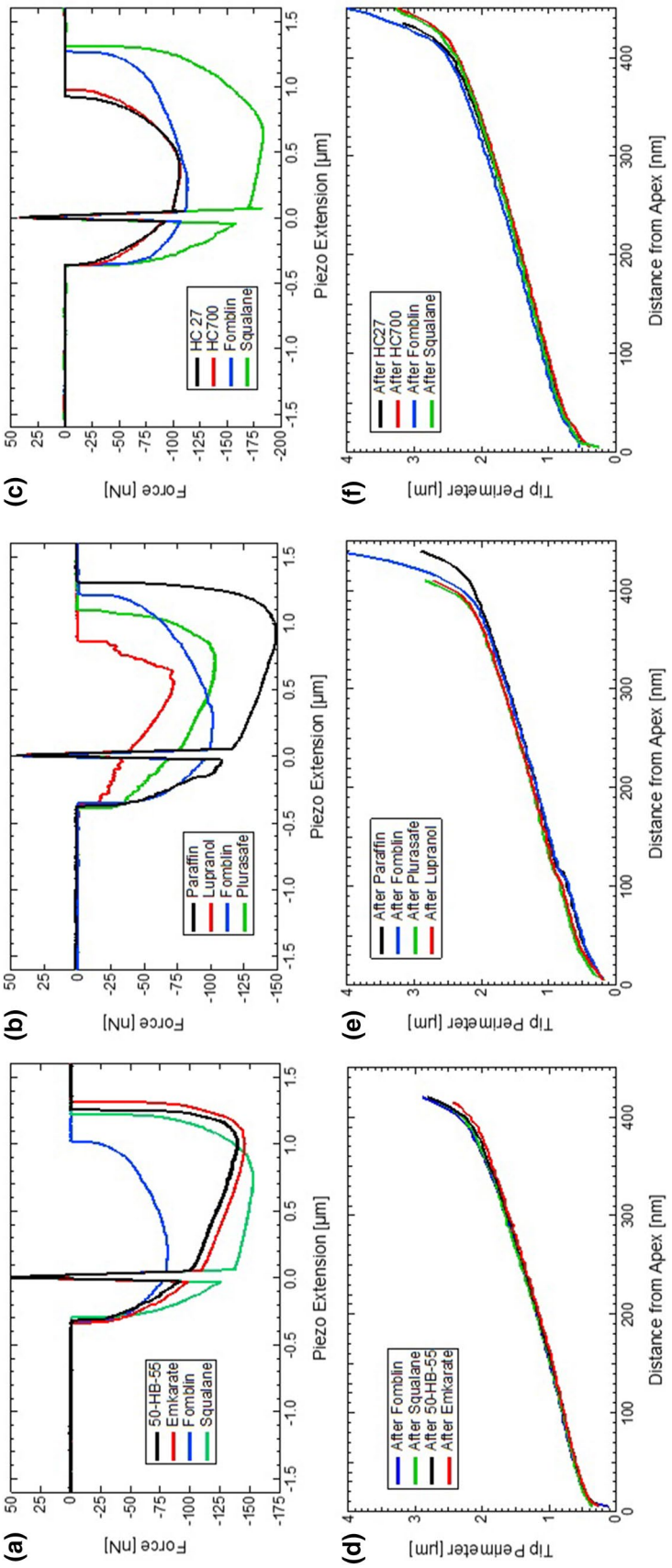

Fig. 3 Force-distance curves with three different tips on films of **a** Fomblin, Squalane, 50-HB-55, and Emkarate, **b** Fomblin, Paraffin, Plurasafe, and Lupranol, and **c** Halocarbon 27, Halocarbon 700, Fomblin, and Squalane. Curves were acquired on films with a thickness of approximately 400 nm. Negative piezo extension corresponds to approach and positive piezo extension corresponds to retraction curves. The perimeters of the cross-section of the respective tips at a certain distance from the apex, acquired by scanning a TGT1 test grating after each force-distance curves measurement, are shown in (**d–f**)

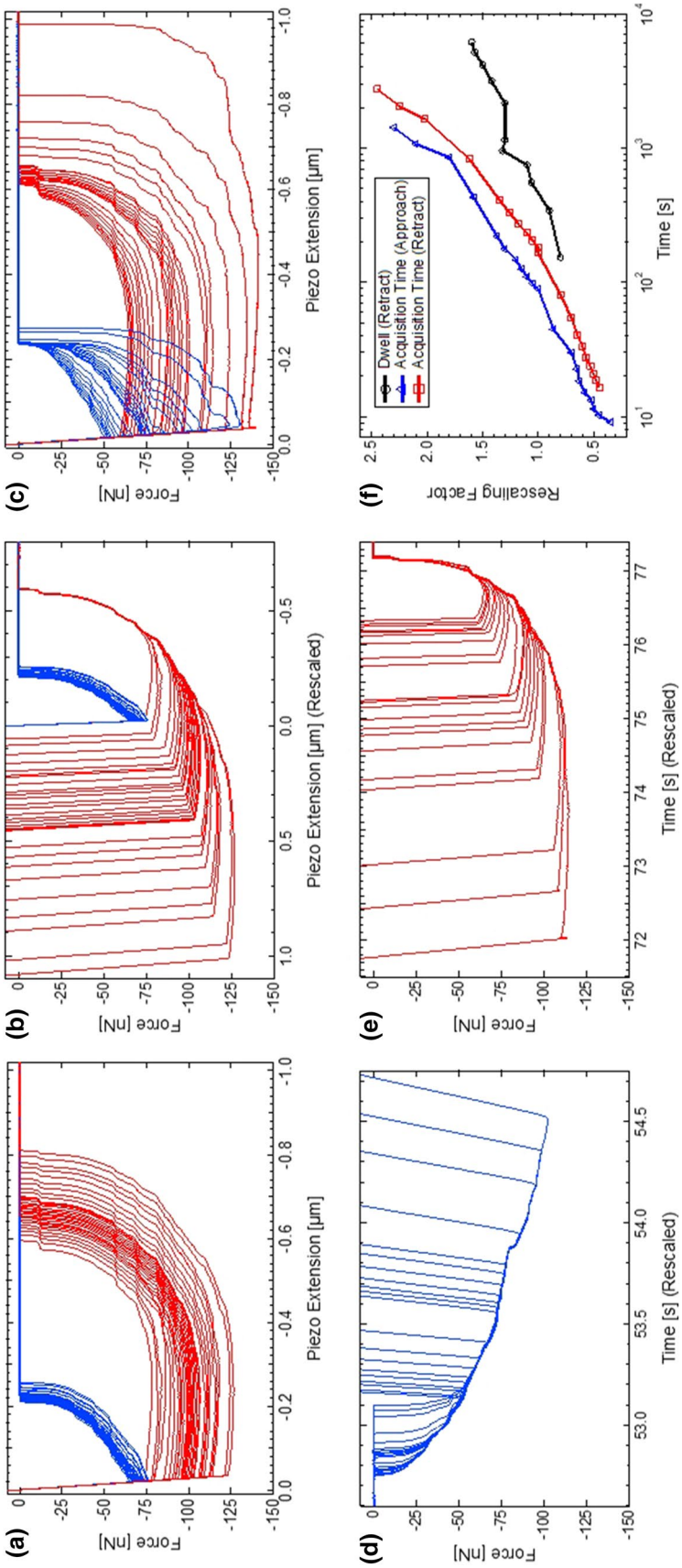

Fig. 4 **a** Approach (blue) and retraction (red) curves on Squalane with dwell times of 0–10 s (curves with larger detachment force from the substrate have longer dwell times). **b** Same curves as in **a**, overlapped after rescaling of the X-axis. **c** Approach (blue) and retraction (red) curves with scan rates of 0.01 to 10 Hz (curves with larger detachment force from the substrate have lower scan rates). **d** Approach curves as in **c**, overlapped after rescaling of the X-axis. **e** Retraction curves as in panel **c**, overlapped after rescaling of the *X*-axis. **f** Rescaling factors of the measurements with varied dwell and acquisition time

(from 65 to 143 nN) and the jump-off-contact occurs at larger distances (from 620 nm to 1 µm) with slower scan rates. Figure 4d, e show that both approach and retraction curves can be overlapped after the time axis has been rescaled. There are however two restrictions. The approach curves do not overlap immediately after the jump-to-contact with the lubricant. This is because of the almost instantaneous building of a meniscus at the tip apex with a velocity which is considerably higher than the subsequent wetting of the tip. The retraction curves, on the other hand, do not overlap in the portion where pinning is present.

The rescaling factors are summarized in Fig. 4f. For the approach curves, they are plotted against the time between the jump-to-contact with the liquid and the onset of the repulsive force when the tip touches the substrate. For the retraction curves, they are plotted against the time between the jump-to-contact and the point when the tip is detached from the substrate again.

The third variable that influences the position of the three-phase contact line is the thickness of the lubricant film. As already discussed, the thickness of the liquid film has been measured throughout this paper only by means of force–distance curves as the distance from the onset of the attractive meniscus force to the onset of the repulsive interaction with the substrate, plus the total bending of the cantilever while penetrating the film. A critical discussion of the accuracy of this method can be found in Refs. [9, 10, 18, 19]. Two factors favor the upward movement of the contact line for thicker films: the thickness of the film itself, as the tip is fully indenting the film, and the longer time the tip spends in the liquid, during which the liquid can climb up the tip. Measurements for a certain lubricant have been performed on a single film with varying thickness. Approach and retraction curves on films of varying thickness can be overlapped after rescaling the *X*-axis, as shown exemplarily for selected curves on Squalane in Fig. 5a, b. Figure 5c shows the rescaling factors, which become larger for thicker films. This means that the curves on thick films must be stretched to overlap with curves on thinner films or, in other words, that the difference between *H* and *S* increases with the film thickness. Indeed, in case of thicker films, the tip spends a longer time in the lubricant, which climbs further along the tip.

After appropriate rescaling, all curves taken with one tip on a specific lubricant, both approach and retraction, do overlap, regardless of dwell time, acquisition time or film thickness (not shown here). This proves indeed that the force acting on the cantilever depends only on the perimeter of the three-phase contact line.

3.2 Differences Between the Lubricants

Because of the obvious differences in the shapes of the curves on different lubricants shown in Fig. 3, it is

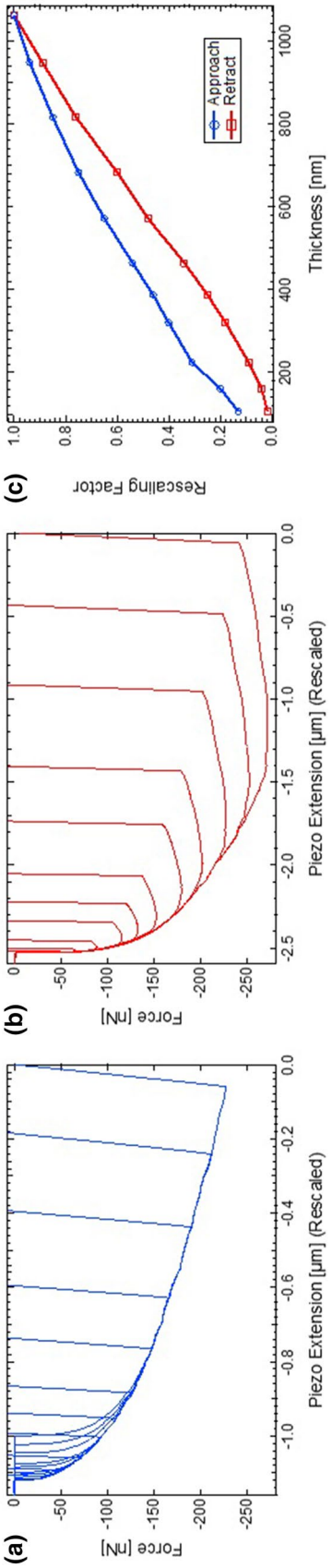

Fig. 5 Rescaled and overlapped force–distance curves acquired on Squalane films of different thickness, **a** approach, and **b** retraction. **c** Rescaling factors

worthwhile to take a closer look at those differences, quantify them and find ways to relate them to the properties of the lubricants. Four different quantities of the force–distance curves on the lubricants used in Fig. 3b are compared in Fig. 6, in dependence of the film thickness. Each curve in Fig. 6 contains data from 225 force curves, providing a dense set of thickness values. The maximum attractive forces when the tip is approached and retracted are shown in Fig. 6a, b, respectively. The largest values are observed for Paraffin, and the lowest for Lupranol. The retraction length, shown in Fig. 6c, is the length of the retraction curve till the jump off contact. It is longer for Paraffin and Fomblin, and shorter for Plurasafe and Lupranol. This means that on Paraffin films the largest force is needed, and the tip must be pulled over the longest distance to remove it from the lubricant. A way to quantify the pinning of the three-phase contact line at the tip is the pinning length, which is illustrated in Fig. 2. The lowest pinning length is observed for Fomblin, which means that the liquid slides off the tip almost immediately after the start of the retraction. Paraffin again shows the highest values. This means that the three-phase contact line remains at its position even after the tip has been withdrawn by large distances, eventually higher than the film thickness itself.

As expected, all those quantities increase with increasing thickness. The increase is almost linear for Lupranol and Plurasafe. For Paraffin and Fomblin, the increase slows down for larger thickness.

To investigate the behavior of different lubricants, the same analysis has been done for the lubricants in Fig. 3c. Fomblin is included again for comparison. The results are shown in Fig. 7. A striking observation is that all four quantities are nearly identical for Halocarbon 27 and Halocarbon 700. Those two substances are chemically the same, but Halocarbon 700 has a significantly higher viscosity. All quantities have their highest values for Squalane.

4 Discussion

The essential parts of a force–distance curve on a lubricant are summarized in Fig. 8. The present section is designed to illustrate those parts, to identify the underlying physical mechanisms and to relate them to the physical properties of the lubricants.

Immediately after the jump-to-contact with the lubricant, a meniscus is formed almost immediately. This becomes apparent in a steep section of the curve, where the attractive force increases very rapidly. All lubricants show this behavior, independently of how well they wet the tip. For

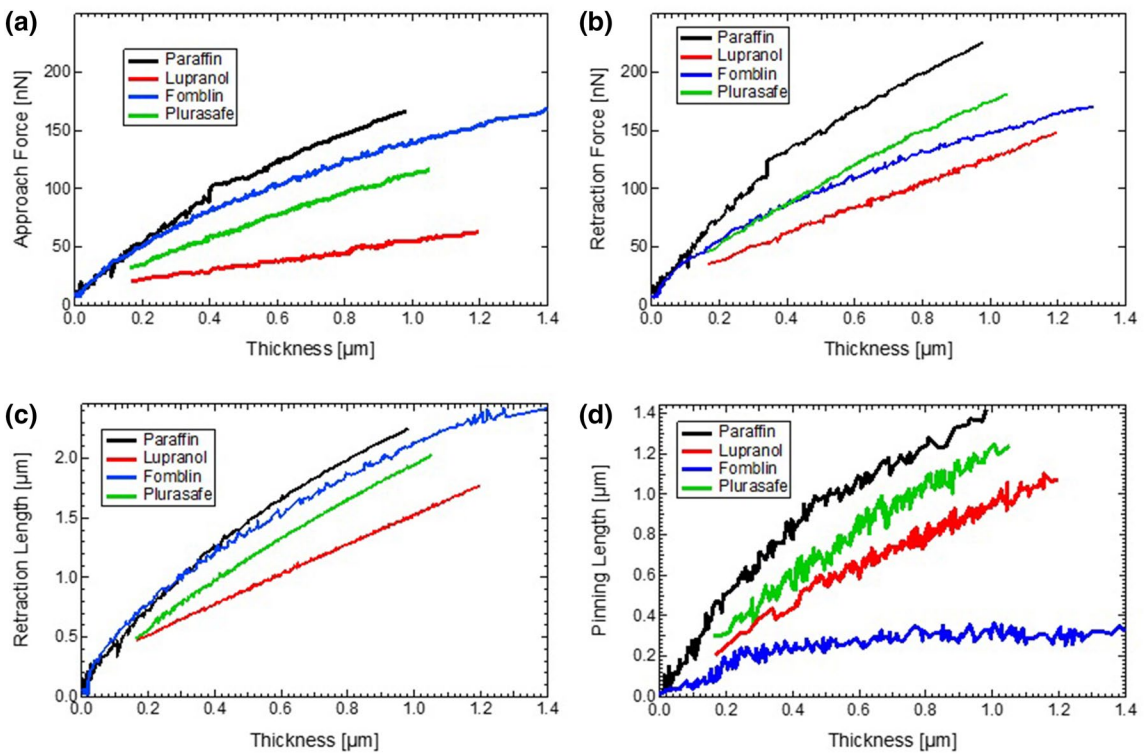

Fig. 6 Maximum approach (**a**) and retraction (**b**) force, retraction length (**c**), and pinning length (**d**) against film thickness for Paraffin, Lupranol, Fomblin, and Plurasafe. All measurements have been done with the same tip, namely the tip used for Fig. 3b, whose perimeter is shown in Fig. 3e

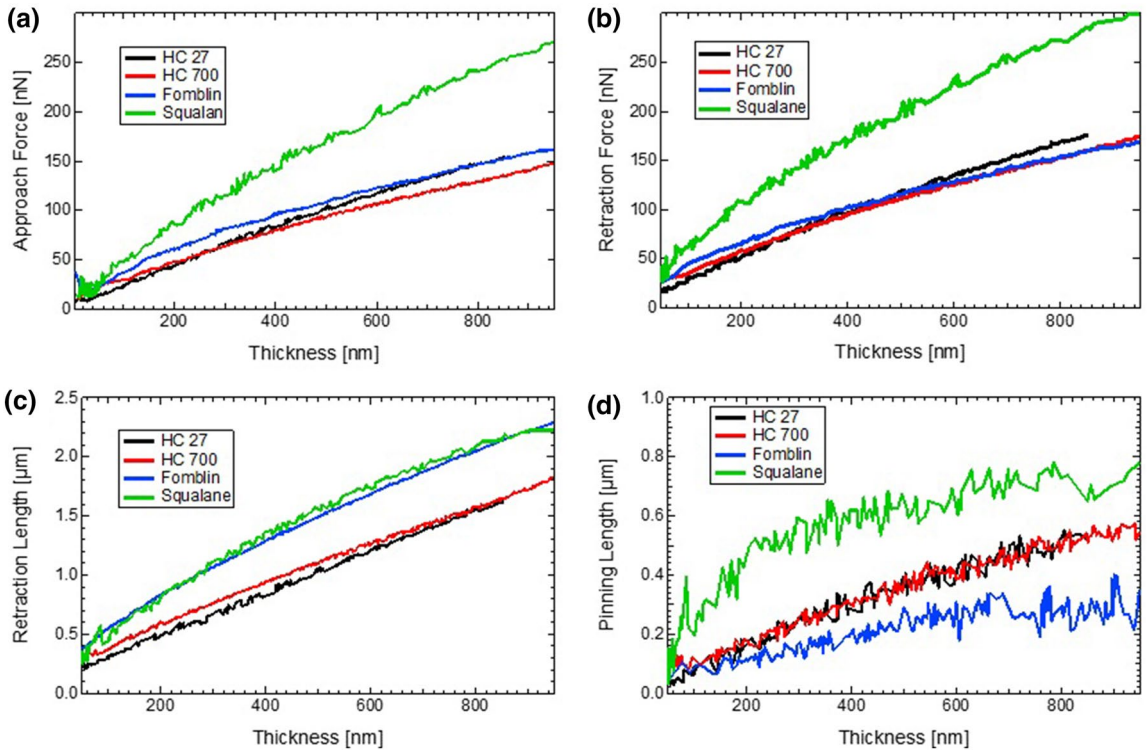

Fig. 7 Maximum approach (**a**) and retraction (**b**) force, retraction length (**c**), and pinning length (**d**) against film thickness for Halocarbon 27, Halocarbon 700, Fomblin, and Squalane. All measurements have been done with the same tip, namely the tip used for Fig. 3c, whose perimeter is shown in Fig. 3f

Lupranol, which exhibits the lowest force (see Fig. 3), this section is very steep. For lubricants exhibiting a higher force, such as Squalane, this section is less steep.

Except for this section immediately after the jump-to-contact, all approach curves can be overlapped if the distance axis is rescaled. This proves that the three-phase contact line moves along the tip with a constant velocity. If the force is divided by $\gamma \sin \alpha$, according to Eq. 1, the resulting quantity is the perimeter of the three-phase contact line. When plotting the perimeter of the three-phase contact line vs the piezo extension or the time, even curves recorded on different lubricants can be overlapped, provided they have been acquired with the same tip. This proves definitely the assumption that the force depends only on the tip perimeter, the surface tension, and the contact angle between lubricant and tip.

Knowing the perimeter of the three-phase contact line at a given distance S between tip apex and rest position of the film, the actual height H of the lubricant on the tip can be calculated. This is possible because the perimeter of the cross-sections of the tip at a given height has been measured (see Fig. 3). Yet, since the test grating tips have a height of ca. 500 nm, this was possible only for heights smaller than ca. 400 nm. For heights larger than ca. 400 nm, a conical tip shape is assumed, and the perimeter has been linearly extrapolated. Figure 9 shows for seven of the nine lubricants H against S at the point where contact with the substrate is established, calculated through curves acquired on films of varying thickness. In this case, S is the thickness of the film. For the sake of clarity, the number of curves has been reduced by omitting the curves of 50-HB-55 and Halocarbon 27, as they are very similar to Paraffin and Halocarbon 700, respectively.

For most lubricants, the assumption that the lubricant climbs up the tip, as shown in Fig. 10a, is confirmed. Yet, the remarkable finding from Fig. 9 is that H is not always larger than S. For Plurasafe and Lupranol, i.e., the curves lying below the dashed gray line with a slope of 1, the three-phase contact line lies below the rest position of the film. However, this does not mean that Plurasafe and Lupranol do not wet the tip. Indeed, their contact angles on silicon are below 40°. Instead, the tip creates a kind of pit or depression in the liquid surface, as illustrated in Fig. 10b. The curve for Emkarate is very close to the dashed line and intersects it for $S \approx 0.6$ µm, as if only thinner films could climb up the tip and thicker films were pushed back. At this stage of the measurements this behavior is not thoroughly understood.

The different wetting behavior is caused by an interplay of surface tension, viscosity, and contact angle. The very small wetted height H for Lupranol can be explained by its

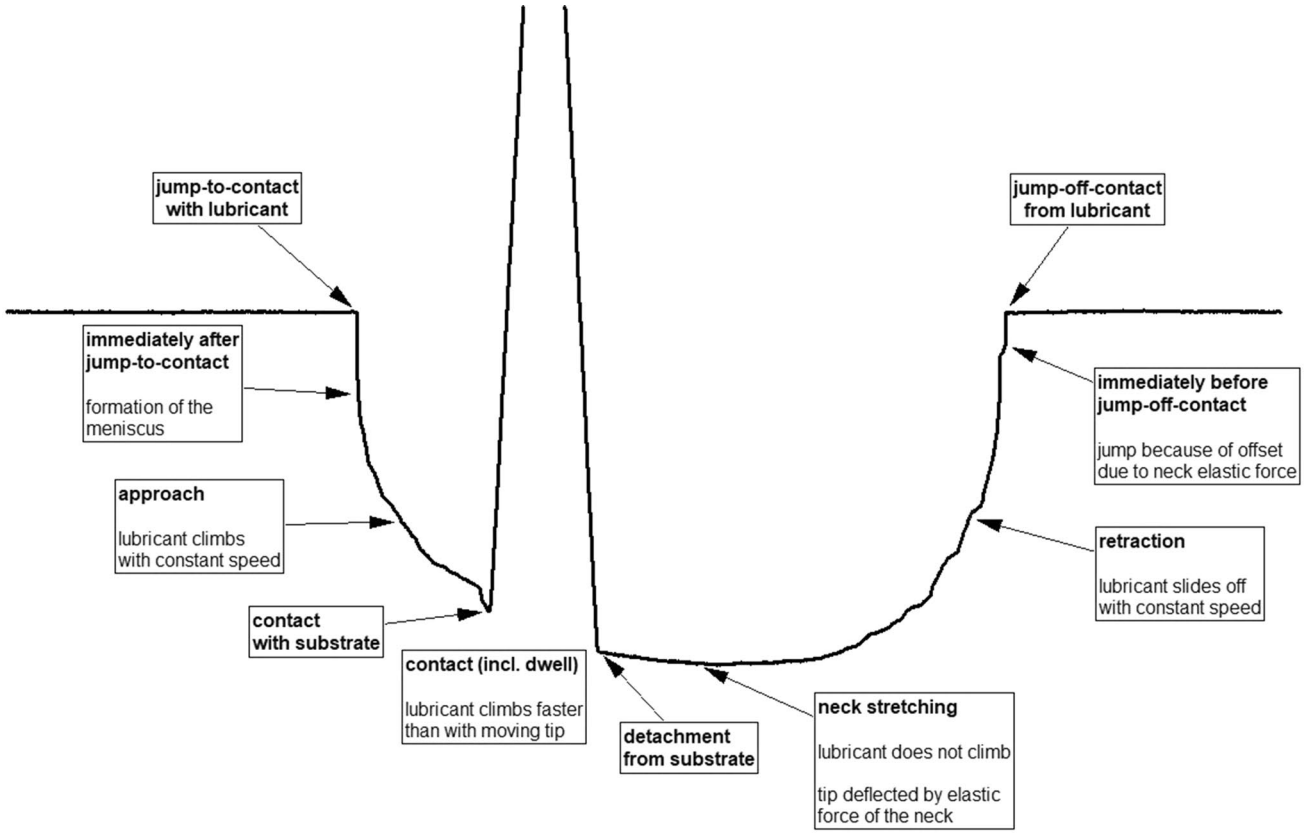

Fig. 8 Synopsis of the essential parts of a force–distance curve on a lubricant

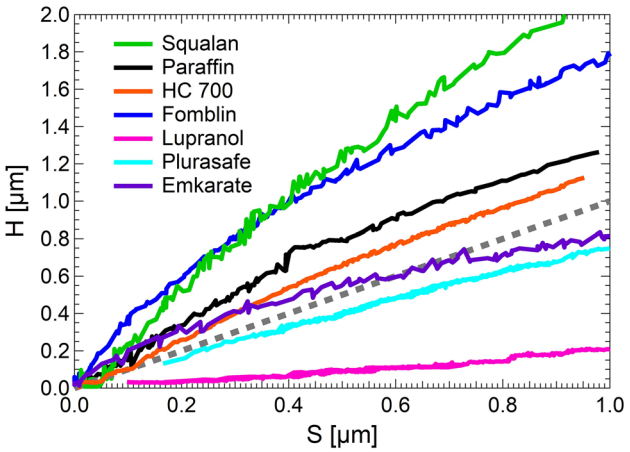

Fig. 9 Height of the lubricant on the tip (*H*) vs. distance between tip apex and rest position of the liquid film (*S*). The dashed grey line has a slope of 1

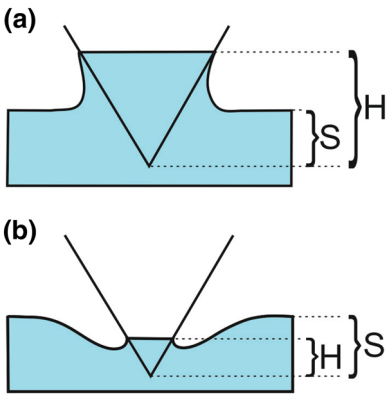

Fig. 10 Illustration of a lubricant climbing up the tip (**a**), and a lubricant being pushed back by the tip (**b**). *H* and *S* are marked in the graphs

very high surface tension, paired with a high viscosity and a comparatively high contact angle. Fomblin, on the other hand, has the lowest surface tension. Therefore, it wets the tip, despite its rather high viscosity. Squalane has a higher surface tension than Fomblin, but a very low viscosity, so it can climb up the tip as well. Measurements with different dwell times have shown that Lupranol hardly climbs during dwell, while Plurasafe climbs significantly, even if its viscosity is almost the double of that of Lupranol. Additionally, Halocarbon 27 and Halocarbon 700 show nearly identical behavior in dwell measurements, although their main difference is the much higher viscosity of Halocarbon 700. Therefore, it can be assessed that the viscosity plays

only a minor role in the climbing of lubricants. This is most probably due also to the fact that the acquisition rate of a force–distance curve is in practice limited to 10 Hz, so that the effect of viscosity is rather small. This analysis shows that liquid properties such as surface tension, viscosity, and contact angle can be used to explain the wetting behavior. Yet, a quantitative analysis requires a much finer variation of the properties and hence a larger set of lubricants.

While the tip is in contact with the substrate, it does not move relative to the sample. This time may be prolonged by an additional dwell time. Measurements with varying dwell time have shown that the lubricant climbs up the tip during this time. Figure 11 shows the capillary force due to the interaction with the lubricant at the beginning and at the end of contact with the substrate vs. the time that the tip has spent in the liquid at this point for measurements on Squalane with varying acquisition time (see Fig. 4b–d). It is evident that, at a certain time, the force at the beginning of the contact with the substrate is smaller than the force at the end, although the tip has spent the same time in the liquid. The reason for this difference is the movement of the tip. Till the beginning of contact with the substrate, the tip has been in downward motion all the time. At the end of contact with the substrate, however, it has rested for a certain time. The lubricant climbs faster when the tip stays still than when the tip moves downward, since the downward movement is opposed to the climbing of the lubricant, which is subsequently hindered by friction.

After the detachment from the substrate, the three-phase contact line is pinned at a certain distance from the tip apex and the meniscus neck is stretched when the tip is retracted. The elastic force resulting from the neck stretching deflects the cantilever further downward. This additional force is not due to the capillary force $F(H) = p(H)\gamma \sin\alpha$ and hence is not related to the position of the three-phase contact line,

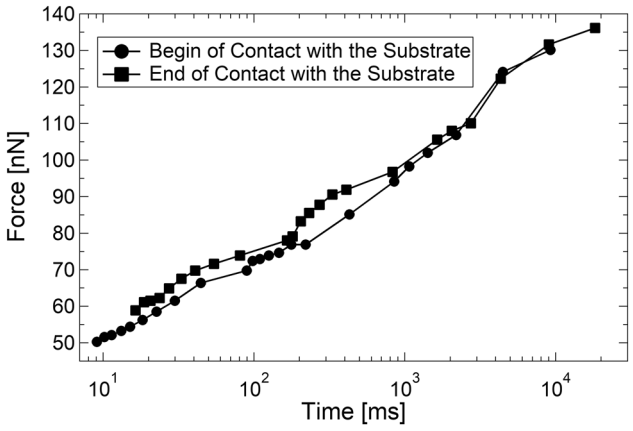

Fig. 11 Force at the beginning and at the end of contact with the substrate vs. time spent in the liquid by the tip for Squalane. The data were obtained from curves with different acquisition times

which indeed does not move. In this regime, the curves can be overlapped without any rescaling, which is a prove for the pinning. Fomblin is the only lubricant that shows almost no pinning. Since Fomblin has the lowest surface energy among the employed lubricants, and since it is known that water, with a very high surface energy, exhibits a very strong pinning, it is reasonable to suppose that high surface energy favors pinning.

When the point of maximal attractive force is reached, and the tip is further retracted, the three-phase contact line begins to recede along the tip. The receding velocity has been found to be constant and to depend on the lubricant. The rescaled curves overlap in this part, analogous to the approach curves. Additionally, approach and retraction curves also overlap with each other. The peculiarity is, however, that the retraction curves must be shifted upward by a distance corresponding to the little jump immediately before the jump-off-contact from the liquid. The reason for this is the additional deflection (or force) experienced by the cantilever during the stretching of the neck. This additional deflection acts like a vertical offset of the retraction curve, so it must be subtracted from the retraction curves to match the approach curves. When the meniscus breaks, the pre-deflection finally disappears, and the force is zero again.

As already stated in the introduction, asperities on surfaces employed in tribological tests can be modeled as an AFM-tip. Asperities play a crucial role in tribological tests, most of all in the running-in regime, i.e. at the beginning of the test, when the surfaces have not yet been flattened through abrasive wear and/or plastic deformation. Our measurements show that, depending on the movement of the tribological partners, some lubricants, e.g. Squalane and Fomblin, do actually wet asperities by climbing on them up to a height, which can be twice as large as the thickness of the lubricant film. Yet, other lubricants, such as Lupranol, wet only a small portion of the asperities, considerably smaller than the thickness of the film itself. This means that, in some cases and with some peculiar lubricants, a lubricated test can be actually partially unlubricated, when considering asperities. As a conclusion, because of the crucial role of asperities in the running-in regime, the efficiency of a lubricant should be always tested also at the nano- and micro-scale.

5 Conclusion

It has been shown that the main results obtained by Cappella for Fomblin [19] are valid also for a large group of lubricants with rather different properties. Force–distance curves recorded with the same tip can be overlapped after a rescaling of the x-axis for all investigated lubricants regardless of dwell time, scan rate, or film thickness. Dividing the force by the material-specific quantities, i.e. $\gamma \sin\alpha$, even enables overlapping curves acquired on different lubricants.

This is a definitive proof that the force acting on a cantilever depends only on the shape of the tip, the surface tension, and the contact angle between lubricant and tip. A next step will be to change the indenter geometry and use colloidal spheres with known geometry instead of tips.

This study has further contributed to the understanding of the different processes during the acquisition of force-distance curves on lubricants. Only parts of the curves where the lubricant moves along the tip with a constant velocity overlap after rescaling. Other parts are dominated by meniscus formation, pinning, or elastic forces caused by the stretching of the liquid neck. Factors such as the occurrence of pinning or the height that the lubricant climbs up the tip are vastly different for the examined lubricants. High surface tension, high viscosity and high contact angle hinder lubricants from climbing the tip. Low surface energy on the other hand prevents pinning. For a detailed understanding of the influence of individual liquid properties on the curve shape, however, a more systematic study on a large array of lubricants is needed.

Acknowledgements The authors thank Mario Sahre, Gundula Hidde, and Andreas Kunzmann for the measurements of the surface tension, contact angle, and viscosity of the lubricants.

Funding Open Access funding enabled and organized by Projekt DEAL.

Compliance with Ethical Standards

Conflict of interest All authors declare that they have no conflict of interest.

References

1. Chung, K.H., Kim, D.E.: Fundamental investigation of micro wear rate using an atomic force microscope. Tribol. Lett. **15**, 135–144 (2003)
2. Wienss, A., Persch-Schuy, G., Vogelgesang, M., Hartmann, U.: Scratching resistance of diamond-like carbon coatings in the sub-nanometer regime. Appl. Phys. Lett. **75**, 1077–1079 (1999)
3. Pidduk, A.J., Smith, G.C.: Scanning probe microscopy of automotive anti-wear films. Wear **212**, 254–264 (1997)
4. Butt, H.-J., Cappella, B., Kappl, M.: Force measurements with the atomic force microscope: technique, interpretation and applications. Surf. Sci. Rep. **59**, 1–152 (2005)
5. Cappella, B., Dietler, G.: Force-distance curves by atomic force microscopy. Surf. Sci. Rep. **34**, 1–104 (1999)
6. Thundat, T., Zheng, X.Y., Chen, G.Y., Warmack, R.J.: Role of relative humidity in atomic-force microscopy imaging. Surf. Sci. Lett. **294**, 939–943 (1993)
7. Thundat, T., Zheng, X.Y., Chen, G.Y., Sharp, S.L., Warmack, R.J., Schowalter, L.J.: Characterization of atomic-force microscope tips by adhesion force measurements. Appl. Phys. Lett. **63**, 2150–2152 (1993)
8. Xiao, X., Qian, L.: Investigation of humidity-dependent capillary force. Langmuir **16**, 8153–8158 (2000)
9. Mate, C.M., Lorenz, M.R., Novotny, V.J.: Atomic force microscopy of polymeric liquid films. J. Chem. Phys. **90**, 7550–7555 (1989)
10. Mate, C.M., Novotny, V.J.: Molecular conformation and disjoining pressure of polymeric liquid films. J. Chem. Phys. **94**, 8420–8427 (1991)
11. Bowles, A.P., Hsia, Y.T., Jones, P.M., Schneider, J.W., White, L.R.: Quasi-equilibrium AFM measurement of disjoining pressure in lubricant nano-films I: Fomblin Z03 on silica. Langmuir **22**, 11436–11446 (2006)
12. Bowles, A.P., Hsia, Y.T., Jones, P.M., White, L.R., Schneider, J.W.: Quasi-equilibrium AFM measurement of disjoining pressure in lubricant nano-films II: effect of substrate materials. Langmuir **25**, 2101–2106 (2009)
13. Brunner, R., Tyndall, G.W., Waltman, R.J., Talke, F.E.: Adhesion between surfaces separated by molecularly thin perfluoropolyether films. Tribol. Lett. **40**, 41–48 (2010)
14. Waltmann, R.J., Guo, X.C.: AFM force-distance curves for perfluoropolyether boundary lubricant films as a function of molecular polarity. Tribol. Lett. **45**, 275–289 (2012)
15. Bao, G.W., Troemel, M., Li, S.F.Y.: AFM study of polymer lubricants on hard disk surfaces. Appl. Phys. A **66**, 1283–1288 (1998)
16. Li, H., Wood, R.J., Endres, F., Atkin, R.: Influence of alkyl chain length and anion species on ionic liquid structure at the graphite interface as a function of applied potential. J. Phys. **26**, 284115 (2014)
17. Krass, M.D., Krämer, G., Dellwo, U., Bennewitz, R.: Molecular layering in nanometer-confined lubricants. Tribol. Lett. **66**, 87 (2018)
18. Ally, J., Vittorias, E., Amirfazli, A., Kappl, M., Bonaccurso, E., McNamee, C.E., Butt, H.-J.: Interaction of a microsphere with a solid-supported liquid film. Langmuir **26**, 11797–11803 (2010)
19. Cappella, B.: Force-distance curves on lubricant films: an approach to the characterization of the shape of the AFM tip. Micron **93**, 20–28 (2017)
20. Hutter, J.L., Bechhoefer, J.: Calibration of atomic-force microscope tips. Rev. Sci. Instrum. **64**, 1868–1873 (1993)
21. Villarrubia, J.S.: Algorithms for scanned probe microscope image simulation, surface reconstruction, and tip estimation. J. Res. Natl. Stand. Technol. **102**, 425–454 (1997)
22. Dongmo, L.S., Villarrubia, J.S., Jones, S.N., Renegar, T.B., Postek, M.T., Song, J.F.: Experimental test of blind tip reconstruction for scanning probe microscopy. Ultramicroscopy **85**, 141–153 (2000)